IEEE Access
Multidisciplinary ⋮ Rapid Review ⋮ Open Access Journal

Received March 12, 2021, accepted March 31, 2021, date of publication April 26, 2021, date of current version June 23, 2021.

Digital Object Identifier 10.1109/ACCESS.2021.3075488

Experimental Study on Pressure Wave Characteristics of High-Voltage Discharge in Water With Hemispherical Electrodes

BIN LI[1], SHENG XUE[1,2], AND LIANG YUAN[1,2]

[1]School of Safety Science and Engineering, Anhui University of Science and Technology, Huainan 232001, China

[2]State Key Laboratory of Mining Response and Disaster Prevention and Control in Deep Coal Mine, Anhui University of Science and Technology, Huainan 232001, China

Corresponding author: Sheng Xue (sheng.xue@aust.edu.cn)

This work was supported in part by the National Natural Science Foundation of China under Grant 51934007.

ABSTRACT High-voltage pulse discharge in water is a promising technology to enhance the permeability of coal seam and rock mass by generating fractures within them. With the aim of improving the stability and efficiency of this technology, a high voltage electric pulse experiment system was constructed. The discharge electrodes in the experiment was hemispherical. The positive and negative electrodes were arranged on the same axis with adjustable spacing. Five sets of experiments were undertaken with the electrode spacing of 1mm, 2mm, 3mm, 4mm, and 5mm, respectively. In the experiments, an oscilloscope was used to analyze the voltage, current, and pressure wave signals. The experimental results of two typical voltage-current curves indicate that the peak pressure of plasma shock wave follows a parabolic trend with the electrode spacing, and there is an optimal electrode spacing for a given discharge voltage. The peak pressure of plasma shock wave tends to increase linearly with the increase of discharge voltage. The greater the electrode spacing, the greater the sensitivity of shock wave peak pressure to the discharge voltage. The shock wave peak pressure sensitivity of 5 mm discharge spacing is 4.7 times that of 1 mm discharge spacing. The experimental results for the voltages of 9 kV, 12 kV, and 24 kV with the optimal electrode spacing show that a power function is the best fit for the attenuation of the peak pressure of shock wave with its propagation distance.

INDEX TERMS Electrodes spacing, plasma shock wave, peak pressure, pressure attenuation, high-voltage discharge in water, hemispherical electrode.

I. INTRODUCTION

In 1938, Yutkin [1] proposed the industrial applications of high voltage electrical pulses. Since then, the high voltage electrical pulse technology has seen significant developments and successful applications in many fields, such as sewage treatment [2], [3], hydraulic electric sand cleaning [4], extracorporeal lithotripsy [5], [6], rock fragmentation [7], oil reservoir removal and fracture creation [8], and new nanomaterial synthesis [9].

In recent years, some scholars [10], [11] put forward the application of high-voltage pulse discharge technology in coal mine gas disaster prevention and control and carried out field tests in some mining areas [12]. In terms of laboratory research, some scholars [13], [14] used the repetitive electrical pulse technology to act on coal, and observed that the pore volume, pore size, micro cracks and other microstructure of the coal increased after the experiment. It was concluded that the high-voltage electrical pulse significantly improved the permeability of coal. Lin *et al.* [15] and Yan *et al.* [16] reached the same conclusion when inserting high voltage electrodes in coal and proposed that the existing fractures and minerals in coal were important factors affecting coal fracturing. In terms of the basic properties of high voltage electrical pulse, Zhu *et al.* [17] concluded through experiments that the liquid conductivity had a major influence on the voltage, current strength, and the pressure wave generated by the discharge, but the shape of electrodes was not mentioned. Lu *et al.* [18] found through experiments that the peak pressure of shock wave was significantly dependent on discharge voltage and electrodes spacing, and the rod electrode with a diameter of 2 mm was selected. Some

The associate editor coordinating the review of this manuscript and approving it for publication was Bernardo Tellini.

scholars [19]–[21] studied the characteristics of the shock wave generated by needle-shaped electrodes and concluded that the deposition energy, plasma channel length, and expansion speed were important contributory factors of the shock wave pressure. In terms of attenuation laws, Liu *et al.* [20] and Zhu *et al.* [22] observed that the shock wave pressure in gas-liquid two-phase medium decreased with the increase of propagation distance. However, the combined effects of electrodes spacing and discharge voltage were yet to be analyzed. In the study of the needle-plate-shaped electrodes, Zhou [23] obtained the relationship between the electrodes spacing, circuit resistance, voltage, and circuit inductance. In terms of applied researches, some scholars suggested the possibility of an optimal electrodes spacing. For example, when removing the Escherichia coli from sewage, researchers [24] found that the shock wave pressure increased first and then decreased as the electrodes spacing increased from 0.25 to 1.5 mm. It was concluded that the pulse arc discharge had the best sewage treatment effect when the electrodes spacing was 1 mm. In the production of rock breaking equipment, researchers [25] found that the selection of electrode spacing is of great significance to the deformation of rock specimen. Some scholars [26]–[28] have studied the effect of metal wire on shock wave performance by adding metal wire between electrodes. Scholars such as Liang [29] and Yang [24] used the electrodes of different shapes to conduct discharge experiments, and found that the relative electrodes of hemispherical tip have better breakdown stability and higher breakdown efficiency. It is clear that the parameters of discharge electrodes play an important role in high voltage pulse discharge experiments. The needle-needle relative electrode, needle-plate relative electrode, and some other forms of electrode have been used in previous studies. However, the research concerning the hemispherical relative electrode with high break down efficiency is few. Therefore, it is necessary to study the discharge characteristics of relative electrode of hemispherical tip.

In this study, a high-voltage pulse discharge experiment was conducted with the relative electrodes of hemispherical tip to investigate the characteristics of the high voltage discharge plasma shock wave and the influences of the discharge electrodes spacing, discharge voltage, and measuring point distance. This study will provide a further theoretical basis for the application of high voltage pulse discharge in rock breaking and coal mass fracturing.

II. HIGH VOLTAGE PULSE DISCHARGE EXPERIMENTAL SYSTEM AND THE PRINCIPLE OF SHOCK WAVE GENERATION

A high-voltage pulse discharge system was built for this study. It mainly consists of a step-up transformer (transformation ratio of 1000:1, the power is 5 kVA), high-voltage rectifier silicon stack, a pulse capacitor (three 5μF withstand voltage of 50kV in parallel), an ignition sphere gap switch, coaxial cable (withstand voltage of 50kV), hemispherical tip discharge electrode with adjustable spacing (adjustable range of 1-5mm), discharge resistance (three 2.1Ω discharge resistor in parallel). A 50kV high-precision pulse high-voltage divider was adopted to measure the capacitor voltage in charging and discharging. A Rogowski coil was utilized to measure the current strength of the charging and discharging circuit. An underwater PCB138 sensor was adopted to measure the shock wave pressure. The experimental data were recorded and collected with an HDO4034 oscilloscope (sampling frequency of 2.5 GHz). The ripple frequency of HVDC in the experiment was 50 Hz, and the ripple coefficient was 0.00175. The maximum DC voltage of the experimental system was 50 kV. The experiment was carried out in a cylindrical container made of Q235 ordinary carbon steel with a diameter of 1.3 m and a height of 0.8 m.

In the related research of rock breaking [7] and fracturing coal [30], it is necessary to put the discharge electrode into the drilled hole of rock or coal in advance. The borehole was also filled with incompressible liquid (water) to ensure low deformation energy loss and high transmission efficiency [31]. Water can spread shock wave mechanical energy very well. Therefore, the experimental container was filled with regular tap water. During the experiment, the hemispherical shaped front end of the electrode can be immersed in water, and the length of the electrode head is 5 cm. The experimental system is shown in Figure 1, the hemispherical tip of the electrode is presented in Figure 2, where d is the distance between the discharge electrodes.

The high voltage charging and discharging experiments were carried out with the system shown in Figure 1. The voltage, current strength, shock wave pressure, and other signals in the process of charging and discharging were monitored during the experiments. It should be noted that two situations would occur when the discharge sphere gap switch T_2 is pressed. One situation is that the energy stored in the capacitor is sufficient, the electric energy will break through the water medium and connect with the discharge circuit to form a plasma channel between the relative electrodes. After the plasma is formed, the water medium will be compressed rapidly to create shock waves with great mechanical energy and transform part of the energy into light energy, sound energy, and radiation energy, etc. The other situation is that the energy stored in the capacitor is not sufficient to break through the water medium between the electrodes. Therefore, the discharge circuit cannot be connected. When all the energy is consumed during the water dielectric breakdown, there will be no current or electric potential in the discharge circuit. At this time, the connected discharge circuit fails to generate plasma and shock waves. The electrodes spacing and the discharge voltage play key roles in both situations.

When the capacitors are charged, turning on the ignition switch will instantaneously apply a high voltage between the electrodes. First, the high-energy electrons will collide with and ionize the water molecules [32], resulting in a pilot flow column [33] that develops from the positive electrode to the negative electrode. As the degree of ionization increases, the temperature between the electrodes and the concentration

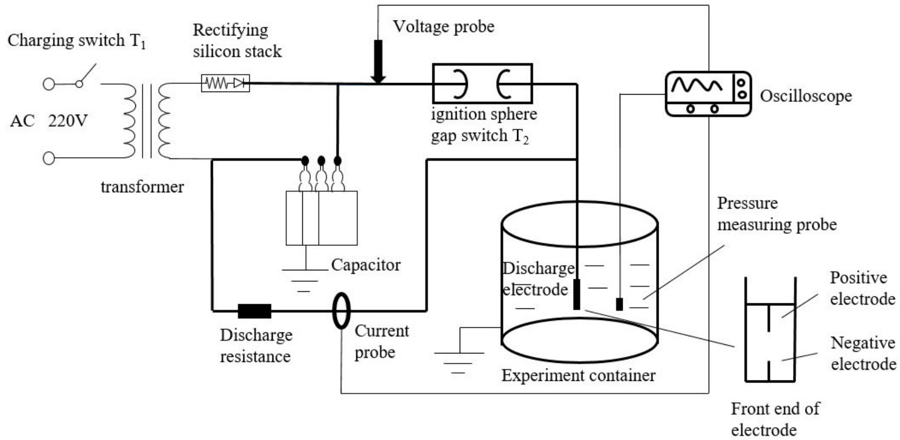

FIGURE 1. Schematic diagram of high-voltage pulse discharge experimental system.

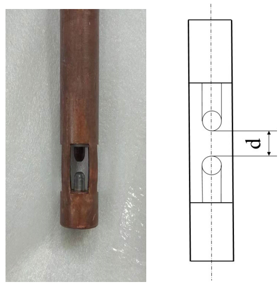

FIGURE 2. A hemispherical shaped electrode. (a) Physical picture of discharge electrode; (b) Structure diagram of discharge electrode.

TABLE 1. Experimental design for optimal electrode spacing.

Combination number	Discharge voltage, U/kV	electrode spacing, d/mm
#1	4	1、2、3、4、5
#2	5	1、2、3、4、5
#3	6	1、2、3、4、5
#4	7	1、2、3、4、5
#5	8	1、2、3、4、5
#6	9	1、2、3、4、5
#7	10	1、2、3、4、5
#8	11	1、2、3、4、5
#9	12	1、2、3、4、5

of ionized particles continue to increase. At the same time, the water molecules change from liquid state to gas state. When the ionization avalanche reaches a certain degree, the electrodes spacing is broken down. Finally, a high-energy, high-temperature and high-density plasma channel is formed. And an arc discharge occurs, which has the characteristics of arc detonation [34], producing a high-energy shock wave.

III. EXPERIMENTAL SCHEME

A. RESEARCH ON OPTIMAL SPACING

In previous studies [20], [24], [25], research on changing the discharge electrodes spacing is involved. In different application fields, the change of electrode spacing produces varied discharge effects. In this study, the plasma shock wave pressure is studied to find the optimal discharge electrodes spacing under different discharge voltage.

The charging voltage values in the experiment were kept under 30 kV to ensure better performance of the pulse capacitors and the safety of the experiments. The electrodes spacing could be adjusted in the range from 1 to 5 mm due to the electrodes structure of the system. A pcb138 pressure sensor was placed at 10 cm away from the discharge center to measure the pressure value of the plasma shock wave. The CH3 channel of the oscilloscope was connected to the pressure sensor to measure the pressure signal. The CH1 channel of the oscilloscope was connected to the circuit voltage signal, and the CH2 channel was connected to the circuit current signal to ensure the synchronous triggering of the three channels and collect data accordingly. The experiment was carried out with varied electrode spacing under each discharge voltage, and the corresponding parameters were measured. The experiment was repeated three times with the same combination. The average pressure value of the pressure sensor was recorded and counted three times. The experiment was conducted 135 times in total. The specific experimental combination mode is shown in Table 1.

B. STUDY ON ATTENUATION LAW OF SHOCK WAVE PRESSURE

The optimal discharge electrodes spacing under each discharge voltage were calculated from the experiments in the previous section. The combinations with discharge voltages below 10 kV and above 10 kV were selected for the further experiments under optimal discharge electrodes spacing to study the attenuation laws of the shock wave pressure. The shock wave pressure at different distances from the discharge center were measured. The discharge voltage was 9 kV, 12 kV, and 24 kV, respectively. The distance between the pressure sensor and the discharge center was 10 cm, 20 cm, 30 cm, 40 cm, and 50 cm, respectively. Each experiment under the same conditions was repeated three times. Average pressure was calculated from the three measurements. A total of 45 experiments were conducted. The specific experimental scheme is presented in Table 2.

TABLE 2. Experimental design for shock wave pressure attenuation.

Combination number	Discharge voltage, U/kV	Pressure test distance, S/cm
#10	9	10、20、30、40、50
#11	12	10、20、30、40、50
#12	24	10、20、30、40、50

IV. EXPERIMENTAL RESULTS

A. TYPICAL VOLTAGE, CURRENT, AND SHOCK PRESSURE WAVEFORMS OF HIGH VOLTAGE PULSE DISCHARGE

The curves of voltage, current strength, and shock wave pressure signals were drawn and two kinds of curves were shown in Figure 3. The first type was obtained in the situation with very little power loss of the system and almost no loss in the forming of voltage and current curve. The second type was obtained in the situation that the power loss of the system is significant. However, for the shock wave pressure curve itself, the peak pressure curves obtained in over 180 experiments are rather similar.

Figure 3 (a) shows the waveform diagram with a discharge voltage of 8kV and the discharge electrodes spacing of 2 mm (experimental combination #5). Figure 3 (b) is the waveform diagram with a discharge voltage of 8kV and the discharge electrodes spacing of 4mm (experimental combination #5). These two kinds of waveforms were drawn from the data measured 10cm away from the discharge center. It can be seen from Figure 3 that when the discharge ignition switch was turned on, it took a certain time to break down the water medium. During the high-voltage discharge, the voltage at both ends of the capacitor dropped rapidly, and the loop current oscillated in an underdamped manner, eventually forming a plasma shock wave. The electromagnetic interference exerted to the pressure sensor when turning on the ignition switch can be observed from the pressure curve. The interference signal was caused by the sudden change of voltage and current strength in the discharge circuit during high voltage breakdown of the water medium. The interference at the moment of breakdown was caused by the strong pulse electromagnetic field generated by the strong current pulse when the plasma channel is formed. These two interference signals can be considered as the information when the ignition switch is turned on and the electrode spacing is broken down.

According to Figure 3 (a), the breakdown occurred approximately 200 μs after the ignition switch was turned on. There was no significant voltage decrease before the breakdown. The peak pressure waveform of shock wave appeared at about 60 μs after the breakdown. As shown in Figure 3 (b), the breakdown occurred approximately 1,900 μs after the spark gap switch was turned on. The voltage dropped significantly before the breakdown. The water medium was not broken down until the voltage dropped from 8 kV to around 4.8 kV. The shock wave pressure peaked approximately 80 μs after the breakdown. The results of the electrical parameters in high voltage discharge experiments are shown in Table 3.

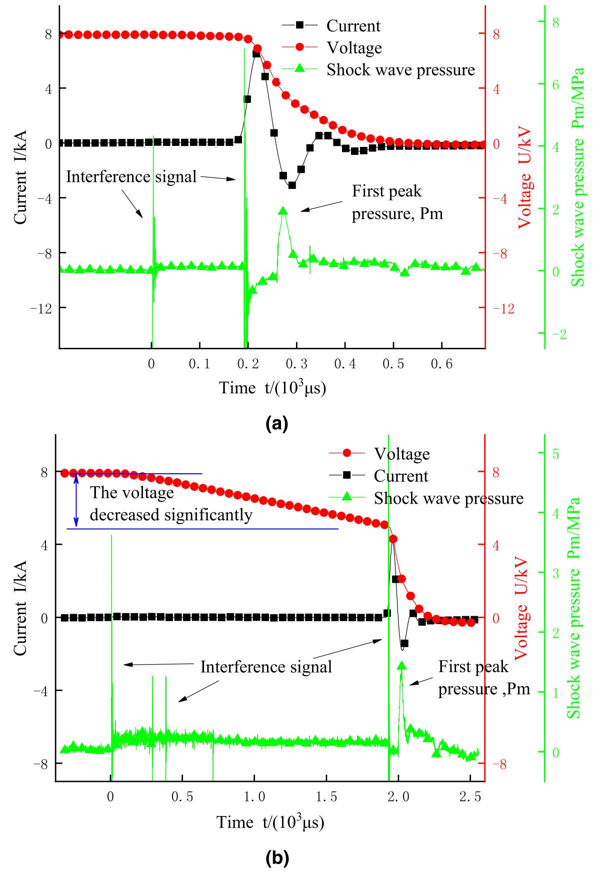

FIGURE 3. Two types of voltage, current, and shock wave pressure curves. (a) The first type; (b) The second type.

B. SHOCK WAVE PRESSURE UNDER DIFFERENT EXPERIMENTAL CONDITIONS

According to the experimental combination in Table 1, the peak pressure of shock wave under different discharge voltage and different discharge spacing can be obtained. The specific peak shock wave pressure is listed in Table 4.

According to the experimental scheme, to study the attenuation law, the experiments were carried out to study the attenuation law at five positions, namely, 10 cm, 20 cm, 30 cm, 40 cm, and 50 cm away from the discharge center were studied combinations, respectively. The aim was to obtain the shock wave pressure at different distances under the three experimental combinations. The values are listed in Table 5.

V. ANALYSIS AND DISCUSSION OF EXPERIMENTAL RESULTS

A. TWO TYPICAL WAVEFORM GENERATION REASONS

The sudden application of a specific high voltage between the two electrodes will change the liquid properties between the electrodes, and the constant change of its resistance value is the most intuitive thing, which will further generate the pulse current. After the generation of the pulse current, the "stream column" [33], like the discharge channel between the electrodes, begins to form and change, eventually forming a plasma shock wave.

TABLE 3. Statistical table of electrical parameters of high voltage discharge experiment.

Discharge voltage U/ kV	Breakdown time t/µs					Voltage drop ΔU/V					Current peak I_{max}/kA				
	1mm	2mm	3mm	4mm	5mm	1mm	2mm	3mm	4mm	5mm	1mm	2mm	3mm	4mm	5mm
4	201.8	-	-	-	-	130	-	-	-	-	3.5	-	-	-	-
5	111.2	1683.8	-	-	-	100	1693.9	-	-	-	4.5	2.8	-	-	-
6	64.8	952.7	2575	-	-	86.7	1186.7	2910	-	-	5.4	4.1	2.5	-	-
7	53.3	510	1181.5	2908.5	-	86.7	720	1670	3615	-	6.0	5.2	4.4	2.7	-
8	33.5	194	837.3	1927.5	-	120	240	1360	3140	-	6.9	6.7	5.8	4.1	-
9	26.8	112.3	390.5	1319.5	2360	120	170	660	2300	4050	7.8	7.6	6.8,	5.6	4.0
10	20.5	112.3	233.5	242.5	1674.8	160	210	400	475	3400	8.8	8.6	7.6	7.7	5.4
11	15	66.7	212	264.5	171	150	186.7	375	490	300	9.7	9.6	9.3	8.6	9.0
12	85.8	53	249.5	143.7	95.8	100	150	466.7	280	160	10.5	10.8	10.2	9.6	9.9

Note: the "-"in the table represents no breakdown and no data.

TABLE 4. Peak pressure of shock wave with various discharge voltages and electrode spacing.

discharge voltage U/kV	Shock wave pressure at different discharge electrode spacing /MPa				
	1mm	2mm	3mm	4mm	5mm
4	0.744	0	0	0	0
5	0.91	0.605	0	0	0
6	1.053	1.252	0.483	0	0
7	1.291	1.426	1.413	0.562	0
8	1.433	1.708	1.821	1.238	0
9	1.615	2.118	2.839	2.752	1.377
10	1.543	2.244	4.092	4.193	3.072
11	1.626	3.176	3.863	4.798	5.419
12	2.049	2.504	3.912	5.765	6.131

Note: the pressure sensor is 10 cm away from the discharge center

After the high voltage is applied to the liquid between the electrodes, the change of the resistance value will become even more complicated [4]. The liquid between the electrodes is a conductor before the breakdown, but after the discharge switch is closed, the liquid will become an insulator immediately, and a specific polarity with a free starting point will be formed with the high electrode [1]. When the free starting point reaches the limit, the two electrodes will be connected. At this time, the electrode spacing is broken down.

Therefore, the distance between the discharge electrodes needs to be adjusted for high-voltage pulse discharge to make better use of the high voltage. The two types of waveforms in the Figure 3 are generated with discharge voltage of 8kV and electrode spacing of 2 mm and 4 mm. It can be seen that the resistance value with electrode spacing of 4mm is larger, which will consume more voltage to connect the discharge circuit. When the electrode spacing was 2 mm, the resistance between the electrode spacing became more appropriate, and a less voltage was consumed to connect with the discharge circuit and generate the shock wave. Similar waveform curves can be obtained with other discharge voltages and electrode spacing. The difference is that the breakdown delay and voltage loss are varied. The differences of breakdown and voltage loss can be observed because the two groups of waveforms have evident contrast. Therefore, these two waveforms are listed accordingly.

B. OPTIMAL SPACING UNDER DIFFERENT DISCHARGE VOLTAGES

Experimental results in Table 4 show the relationship between the shock wave pressure obtained with different discharge electrode spacing under the voltage from 4 to12 kV. It can be seen that the shock wave pressure under a particular discharge voltage varies with the discharge electrode spacing. When electrical energy is applied to the discharge electrodes, the energy deposited between discharge electrodes will break through the electrode spacing before forming a plasma shock wave [35]. Pulse energy between the electrode spacing is important [33], which determines the peak pressure of the shock wave. Different electrode spacing has different pulse energy, thus, different electrode spacing eventually can change the peak pressure of the shock wave.

The relationship between the first peak shock wave pressure and the different discharge electrodes spacing is plotted in Figure 4 according to Table 4.

Figure 4 is the curve fitting diagrams of the three types of shock wave peak pressure with significant characteristics. Figure 4 (a) shows the fitting curve when the discharge voltage was 4 kV and 5 kV, indicating that when the discharge electrodes spacing was larger than 2mm under 4kV or 3mm under 5 kV, the liquid medium cannot be broken down. This shows that with a constant initial electric energy, the range of electrodes spacing suitable for liquid medium breakdown is rather limited. It can be observed from the fitting curves of 4kV and 5kV that the peak shock wave pressures decreased with the increase of discharge electrodes spacing, showing the shape of the right side of an inverted parabola.

Figure 4 (b) shows the fitting curve of discharge voltages from 6 to 10 kV, in which shock wave was detected at the discharge electrodes spacing of 1mm, 2mm, and 3mm under a discharge voltage of 6kV. The shock wave pressure when the discharge electrodes spacing was 2mm was higher than that of 1mm or 3mm. However, when the electrode spacing was 4mm or 5mm, the water medium cannot be broken down. Therefore, under a discharge voltage of 6kV, the shock wave pressure increased first and then decreased with the increase of discharge electrodes spacing. When the discharge voltage was 7kV, 8kV, 9kV, and 10kV, the shock wave pressure increased first and then decreased with the increase of discharge electrodes spacing, showing the shape of an inverted parabola.

According to Figure 4 (c), when the discharge voltages were 11kV and 12kV, the shock wave pressure increased with the increase of discharge electrodes spacing. The peak pressure of the shock wave and the discharge electrode spacing

TABLE 5. The shock wave pressure at various propagation distance with optimal electrodes spacing.

Discharge voltage, U/kV	Discharge electrode spacing, d/mm	Shock wave pressure at different distances , Pm/MPa				
		10cm	20cm	30cm	40cm	50cm
9	3	2.839	1.389	1.04	0.426	0.439
12	5	6.131	2.1	1.58	1.03	1.27
24	5	11.77	4.81	3.71	2.56	1.96

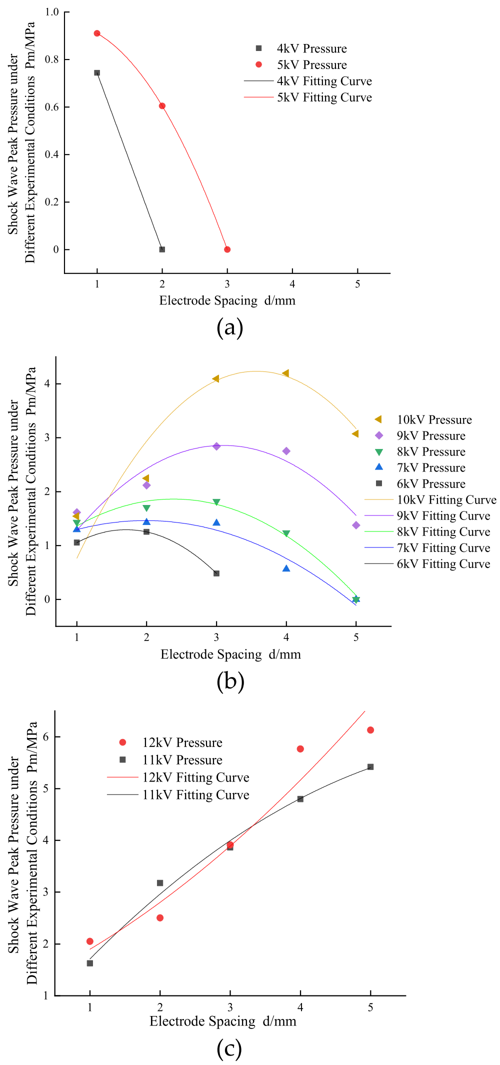

FIGURE 4. The relationship between the first peak pressure and discharge electrode spacing. (a) Discharge voltage of 4kV and 5kV; (b) Discharge voltage from 6kV and 10kV; (c) Discharge voltage of 11kV and 12kV.

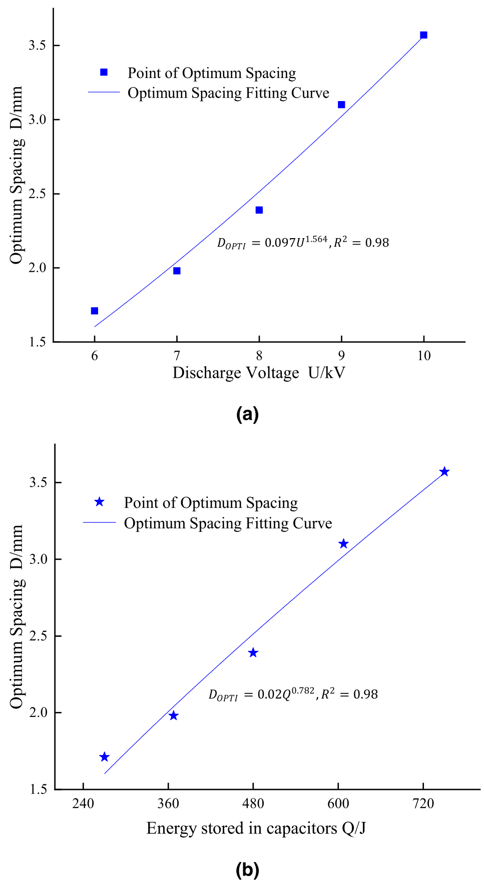

FIGURE 5. (a). The optimal electrode spacing with the discharge voltage. (b). The optimal electrode spacing with capacitor energy.

TABLE 6. The optimal electrode spacing with discharge voltage.

discharge voltage U/kV	Capacitance C/μF	capacitor energy Q/J	optimal electrode spacing d/mm
6	15	270	1.71
7	15	367.5	1.98
8	15	480	2.39
9	15	607.5	3.1
10	15	750	3.57

exhibit the characteristics of the left side of an inverted parabola.

Figure 4 shows that there is an optimal discharge electrode spacing under each initial discharge energy, and there is an apparent ''parabola'' characteristic between the peak pressure of the shock wave and the discharge electrode spacing, which is consistent with the previous study [24], [33], [36]. The shock wave pressure peaked under optimal discharge electrodes spacing. Note that this conclusion is only suitable for discharge voltages ranging from 6kV to 10kV because the maximum electrode spacing of the experimental is 5mm.

The optimal electrode spacing is defined as the discharge electrode spacing of the peak shock wave pressure corresponding to each discharge voltage. According to Figure 4 (b), the optimal discharge spacing under the corresponding discharge voltage is shown in Table 6.

The fitted curve of optimal discharge electrodes spacing D_{OPTI} and discharge voltage U and the fitted curve of D_{OPTI} and capacitor energy storage Q in Table 6 is presented in Figure 5.

The relationship between D_{OPTI} and discharge voltage U is that $D_{OPTI} = 0.097 \cdot U^{1.564}$, $R^2 = 0.98$; and that between D_{OPTI} and capacitor energy Q is that $D_{OPTI} = 0.02Q^{0.782}$, $R^2 = 0.98$. In this system, the capacitance is $15\mu F$.

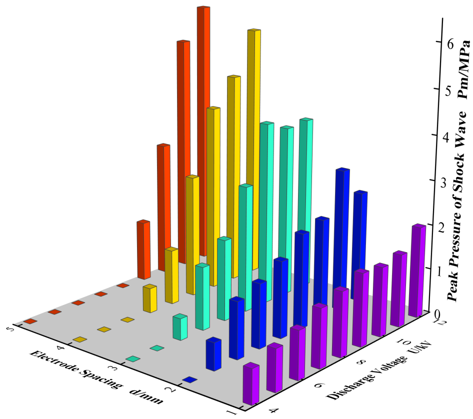

FIGURE 6. Relationship between the first peak pressure and discharge voltage.

Further investigations are needed for different capacitances. The empirical formula is in line with the formula for estimating electrode spacing proposed by Liu Ning [25] except that the ratio coefficient and power function coefficient of the two are different. It can be concluded that the ratio coefficient and power function coefficient are determined by the specific structure of the electrode and the characteristics of the equipment. The basic formula can be written as $D_{OPTI} = \alpha \cdot U^{\theta}$.

When the discharge voltage was 4kV and 5kV, the optimal electrode spacing was 1mm. When the discharge voltage was 11kV and 12kV, the optimal electrode spacing was 5mm. It can be inferred that when the discharge voltage is larger than 10kV, the optimal electrode spacing in the experimental system is 5mm.

C. THE RELATIONSHIP BETWEEN THE PEAK PRESSURE OF SHOCK WAVE AND THE DISCHARGE VOLTAGE WITH THE SAME ELECTRODE SPACING

With constant discharge electrodes spacing, the changes in peak shock wave pressure under different discharge voltage can be obtained according to the experimental results in Table 4.

As can be seen from Figure 6, with the same discharge electrode spacing, the electrode spacing will be broken down as long as the initial discharge energy is large enough or the discharge voltage is high enough. In this case, the probability of peak pressure of shock wave increasing with the rise of discharge voltage is higher than 85%, and the relationship between peak pressure of first shock wave and discharge voltage is almost linear. The larger the electrode spacing, the higher the required initial energy or discharge voltage.

With different electrode spacing, the changing rate K of the peak shock pressure is calculated spacing with the increase rise of the discharge voltage in Table 7. Table 7 shows the relationship between the increase of peak shock pressure with different discharge electrode spacing as the discharge voltage increases from 4 kV to 12kV. It can be clearly seen from Table 7 that the increment of peak pressure rises with the electrode spacing. As the spacing increase from 1 mm to 5 mm, the pressure increment rises from 1.305 MPa to

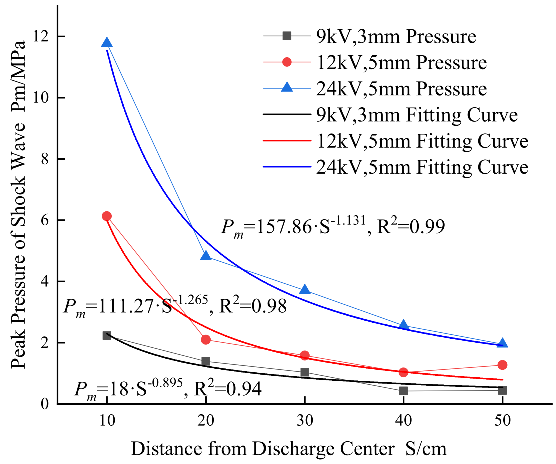

FIGURE 7. Attenuation diagram of peak pressure with propagation distance at optimal spacing.

TABLE 7. The changing rate of peak pressure with discharge voltage with different electrode spacing.

electrode spacing, d/mm	Pressure increase, ΔP_m/MPa	Discharge voltage increase, ΔU/kV	Rate of change, K
1	1.305	8	0.163
2	2.504	8	0.313
3	3.912	8	0.489
4	5.765	8	0.721
5	6.131	8	0.766

6.131 MPa. When the electrodes spacing was 1mm, 2mm, 3mm, 4mm, and 5mm, the increasing rate of the peak pressure with the increase of the discharge voltage were recorded as K1, K2, K3, K4, and K5. It is safe to conclude that K1<K2<K3<K4<K5, and K5 is approximately 4.7 times of K1. Thus, the larger the discharge electrodes spacing, the greater the changing rate of the peak shock wave pressure with the increase of the discharge voltage. That might be due to the increase in resistance and stored energy between the electrodes with the increase in the electrode spacing.

The pressure of the plasma shock wave increases linearly with increase of the discharge voltage, but the energy storage capacity of the system is constant. Taking safety and cost into consideration, it is impractical to blindly improve the discharge voltage. Therefore, a reasonable discharge voltage is needed for the high voltage discharge experiments.

D. ANALYSIS OF THE ATTENUATION LAW OF SHOCK WAVE PRESSURE WITH PROPAGATION DISTANCE UNDER THE OPTIMAL ELECTRODE SPACING

In the experimental system, the maximum distance between electrodes is 5mm, which is also the optimal electrode spacing when the discharge voltage is greater than 10kV. Three experiments were conducted out with the voltage under 10kV and above 10kV to study the attenuation law, where, the optimal electrode spacing of 9 kV discharge voltage is 3 mm, the optimal electrode spacing of 12 kV and 24 kV are 5 mm. According to the experimental results listed in Table 5, the relationship between the peak pressure of shock wave and the distance between measuring points under the optimal spacing was plotted in Figure 7. Regression analysis was also conducted for the three measuring points. Furthermore, the fitting curve of the shock wave pressure and the distance between the measuring points under the optimal electrodes spacing is shown in Figure 7.

It can be seen from Figure 7 that the peak pressure of the shock wave decreases continuously with the increase of propagation distance under all three discharge voltages. The fitting curve shows that the shock wave pressure Pm changes with the propagation distance S in a power function, and the correlation coefficients are all larger than 0.94. The reason is that the shock wave is an energy consuming process with energy transformation. During propagation, the shock wave reflects and refracts upon the container wall or other objects, which eventually exhaust mechanical energy of the shock wave.

Under the optimal spacing of the three discharge voltages, the fitting relationship between the peak pressure Pm and the propagation distance L is as follows:

When the spacing is 3 mm, and the voltage is 9 kV, $P_m = 18 \cdot S^{-0.895}$;

When the spacing is 5 mm, and the voltage is 12 kV, $P_m = 111.27 \cdot S^{-1.265}$;

When the spacing is 5 mm, and the voltage is 24 kV, $P_m = 157.86 \cdot S^{-1.131}$.

This conclusion is consistent with the findings of previous studies [4], [37], and the primary form of the empirical formula on the attenuation law obtained is a power function relationship.

It is necessary to combine the electrodes spacing and the discharge voltage reasonably for optimal use of the high voltage pulse discharge. The peak pressure of shock wave increases with the increase of stored pulse energy [19]. A higher discharge voltage often produces a greater shock wave pressure. However, excessively high voltages are not recommended due to the energy storage capacity, cost, and safety of the system. Therefore, the discharge voltage and electrode spacing should be combined reasonably to achieve the ideal shock wave pressure and then make the best use of this shock wave mechanical energy.

VI. CONCLUSION

The basic research on the shock wave generated by high voltage pulse discharge under water is very important for its applications in many fields. In this experimental study, the characteristics of shock waves generated with hemispherical discharge electrodes were investigated and the following conclusions were drawn:

1. The high-efficiency application of high-voltage pulse technology requires a reasonable combination of discharge voltage and discharge spacing.
2. There is an optimal discharge electrode spacing (D) for each discharge voltage (U) or capacitor energy (Q). The empirical formula of the optimal discharge electrode spacing is $D_{OPTI} = 0.097U^{1.564}$ and $D_{OPTI} = 0.02Q^{0.782}$, which are suitable for the hemispherical relative electrode. The formulas are consistent with the empirical formulas of the needle-needle relative
3. As long as the electrodes spacing is suitable for the breakdown of the liquid medium, higher discharge voltages are favorable to the peak shock wave pressure most of the time.
4. The larger the electrode spacing, the greater the sensitivity of the plasma shock wave peak pressure to the discharge voltage. At large electrodes spacing, an increased discharge voltage accelerates the increase of the peak shock wave pressure. The sensitivity of peak shock wave pressure to the increase of discharge voltage when the discharge electrodes spacing is 5 mm is 4.7 times that of 1 mm.
5. In the discharge experiment with the optimal electrode spacing, the attenuation law for the peak pressure of the shock wave with the propagation distance conforms to the power function relationship.

REFERENCES

[1] L. Yutkin, "Phenomena near discharge region in liquid," in *Electrohydraulic Effect*, 1st ed. Beijing, China: Science Press, 1962, pp. 3–5.

[2] S. Krishna, A. Maslani, T. Izdebski, M. Horakova, S. Klementova, and P. Spatenka, "Degradation of verapamil hydrochloride in water by gliding arc discharge," *Chemosphere*, vol. 152, pp. 47–54, Jun. 2016, doi: 10.1016/j.chemosphere.2016.02.083.

[3] E.-J. Lee, W. Lee, M. Kim, E. H. Choi, and Y.-J. Kim, "Arc discharge-mediated disassembly of viral particles in water," *Water Res.*, vol. 102, pp. 305–312, Oct. 2016, doi: 10.1016/j.watres.2016.06.052.

[4] K.-J. Chung, S.-G. Lee, Y. S. Hwang, and C. Y. Kim, "Modeling of pulsed spark discharge in water and its application to well cleaning," *Current Appl. Phys.*, vol. 15, no. 9, pp. 977–986, Sep. 2015, doi: 10.1016/j.cap.2015.05.010.

[5] C. Chaussy, W. Brendel, and E. Schmiedt, "Extracorporeally induced destruction of kidney stones by shock waves," *Lancet*, vol. 2, no. 8207, pp. 1265–1268, 1980, doi: 10.1016/S0140-6736(80)92335-1.

[6] M. Basulto-Martínez, I. Klein, and J. Gutiérrez-Aceves, "The role of extracorporeal shock wave lithotripsy in the future of stone management," *Current Opinion Urol.*, vol. 29, no. 2, pp. 96–102, Mar. 2019, doi: 10.1097/MOU.0000000000000584.

[7] D. Bian, J. Zhao, S. Niu, and J. Wu, "Rock fracturing under pulsed discharge homenergic water shock waves with variable characteristics and combination forms," *Shock Vib.*, vol. 2018, no. 4, pp. 1–11, 2018.

[8] W. Chen, O. Maurel, T. Reess, A. S. De Ferron, C. La Borderie, G. Pijaudier-Cabot, F. Rey-Bethbeder, and A. Jacques, "Experimental study on an alternative oil stimulation technique for tight gas reservoirs based on dynamic shock waves generated by pulsed arc electrohydraulic discharges," *J. Petroleum Sci. Eng.*, vols. 88–89, pp. 67–74, Jun. 2012, doi: 10.1016/j.petrol.2012.01.009.

[9] C. G. Kaufmann, Jr., R. Y. S. Zampiva, M. J. Anzanello, A. K. Alves, C. P. Bergmann, and S. R. Mortari, "One-step synthesis of carbon nanoflowers by arc discharge in water," *Ceram. Int.*, vol. 46, no. 16, pp. 26229–26232, 2020, doi: 10.1016/j.ceramint.2020.07.071.

[10] A. Qiu, Y. Zhang, B. Kuai, X. Lv, and J. Tang, "The idea of high power pulse technology applied in unconventional natural gas development," in *Proc. 2nd Energy Forum Chin. Acad. Eng.* Beijing, China: National Energy Administration, Nov. 2012, pp. 1112–1124.

[11] Y. Qin, A. Qiu, and Y. Zhang, "Experiment and discovery on permeability improved technology of coal reservoir based on repeated strong pulse waves of high energy accumulation," *Coal Sci. Technol.*, vol. 42, no. 6, pp. 1–7, 2014, doi: 10.13199/j.cnki.cst.2014.06.001.

[12] Y. Zhang, Z. Meng, Q. Yong, Z. Zhifeng, Y. Zhao, and A. Qiu, "Innovative practice of controllable shock wave in soft coal seam to increase transmission of gas drainage—Taking Zhongjing coal mine in Shuicheng mining area, Guizhou as an example," *J. China Coal Soc.*, vol. 44, no. 8, pp. 2388–2400, 2019, doi: 10.13225/j.cnki.jccs.KJ19.0508.

[13] H. Li, Y. Qin, Y. Zhang, Q. Shi, and X. Zhou, "Experimental study on the effect of strong repetitive pulse shockwave on the pore structure of fat coal," *J. China Coal Soc.*, vol. 40, no. 4, pp. 915–921, 2015, doi: 10.13225/j.cnki.jccs.2014.1528.

[14] Q. Shi, Y. Qin, H. Li, A. Qiu, Y. Zhang, X. Zhou, and S. Zheng, "Response of pores in coal to repeated strong impulse waves," *J. Natural Gas Sci. Eng.*, vol. 34, pp. 298–304, Aug. 2016, doi: 10.1016/j.jngse.2016.06.067.

[15] B. Lin, X. Zhang, Y. Li, and C. Zhu, "Experiment and simulation of selective cracking of coal samples by plasma," *J. China Coal Soc.*, vol. 44, no. 11, pp. 3472–3479, 2019, doi: 10.13225/j.cnki.jccs.2019.0109.

[16] F. Yan, B. Lin, C. Zhu, C. Guo, Y. Zhou, Q. Zou, and T. Liu, "Using high-voltage electrical pulses to crush coal in an air environment: An experimental study," *Powder Technol.*, vol. 298, pp. 50–56, Sep. 2016, doi: 10.1016/j.powtec.2016.05.023.

[17] L. Zhu, Z.-H. He, Z.-W. Gao, F.-L. Tan, X.-G. Yue, and J.-S. Chang, "Research on the influence of conductivity to pulsed arc electrohydraulic discharge in water," *J. Electrostatics*, vol. 72, no. 1, pp. 53–58, Feb. 2014, doi: 10.1016/j.elstat.2013.11.004.

[18] X. Lu, Y. Pan, and H. Zhang, "The electrical and acoustical characteristics of pulsed discharge in water," *Acta Phys. Sinica*, vol. 51, no. 7, pp. 1549–1553, 2002, doi: 10.3321/j.issn:1000-3290.2002.07.024.

[19] X. Y. Li; Liu, Z. Li, G. Zhou, Q. Zhang, F. Lin, and Y. Pan, "Observation of underwater pulse discharge and influence of deposited energy on shock wave in non-uniform electric field," *Proc. CSEE*, vol. 37, no. 10, pp. 3028–3036, 2017, doi: 10.13334/j.0258-8013.pcsee.160315.

[20] Y. Liu, Z. Li, X. Li, G. Zhou, H. Li, Q. Zhang, and F. Lin, "Energy transfer efficiency improvement of liquid pulsed current discharge by plasma channel length regulation method," *IEEE Trans. Plasma Sci.*, vol. 45, no. 12, pp. 3231–3239, Dec. 2017, doi: 10.1109/TPS.2017.2651105.

[21] Y. Liu, Z. Li, X. Li, G. Zhou, Q. Zhang, F. Lin, and Y. Pan, "Effect factors of the characteristics of shock waves induced by underwater high current pulsed discharge," *Proc. CSEE*, vol. 37, no. 9, pp. 2741–2750, 2017, doi: 10.13334/j.0258-8013.pcsee.160417.

[22] L. Zhu, Q. Huang, Y. Xu, Q. Lin, Z. Liu, and Z. He, "Experimental research on pressure waves of pulse arc electrohydraulic discharge," *High Voltage Eng.*, vol. 41, no. 10, pp. 3518–3522, 2015, doi: 10.13336/j.1003-6520.hve.2015.10.046.

[23] G. Zhou, "Study on influence of shock waves induced by underwater pulse current discharges," M.S. thesis, School Elect. Electron. Eng., Huazhong Univ. Sci. Technol., Wuhan, China, 2018.

[24] J. Yang, Z. He, Y. Liu, Z. Zhang, Z. Tu, and M. Yin, "Effects of electrode parameters on sewage disinfection by underwater pulsed arc discharge," *J. Electrostatics*, vol. 98, pp. 34–39, Mar. 2019, doi: 10.1016/j.elstat.2019.01.005.

[25] N. Liu, "Study on electro-hydraulic impulse water jet generator and rock-breaking," M.S. thesis, School Mech. Eng., Chongqing Univ., Chongqing, China, 2008.

[26] R. Han, J. Wu, W. Ding, H. Zhou, A. Qiu, and Y. Zhang, "Characteristics of underwater electrical explosion of a copper wire under different pulsed currents," *Proc. CSEE*, vol. 39, no. 4, pp. 1251–1259, 2019, doi: 10.13334/j.0258-8013.pcsee.172497.

[27] L. Li, D. Qian, X. Zou, and X. Wang, "Effect of deposition energy on underwater electrical wire explosion," *IEEE Trans. Plasma Sci.*, vol. 46, no. 10, pp. 3444–3449, Oct. 2018, doi: 10.1109/TPS.2018.2811124.

[28] A. Rososhek, S. Efimov, V. Gurovich, A. Virozub, S. Tewari, and Y. Krasik, "Evolution of a shock wave generated by underwater electrical explosion of a single wire," *Phys. Plasmas*, vol. 26, no. 4, pp. 1–7, 2019, doi: 10.1063/1.5092321.

[29] M. Liang, "Study on pulsed arc discharge in water and its pressure wave characteristics," M.A. thesis, School Elect. Electron. Eng., Huazhong Univ. Sci. Technol., Wuhan, China, 2017.

[30] H. Lu, "Experimental research on fracturing coal with high-voltage electrical pulse," Ph.D. dissertation, School Resour. Saf. Eng., China Univ. Mining Technol., Beijing, China, 2015.

[31] Q. Ye, Z. Jia, and C. Zheng, "Study on hydraulic-controlled blasting technology for pressure relief and permeability improvement in a deep hole," *J. Petroleum Sci. Eng.*, vol. 159, pp. 433–442, Nov. 2017, doi: 10.1016/j.petrol.2017.09.045.

[32] M. M. Mann, A. Hustrulid, and J. T. Tate, "The ionization and dissociation of water vapor and ammonia by electron impact," *Phys. Rev.*, vol. 58, no. 4, pp. 340–347, Aug. 1940, doi: 10.1103/PhysRev.58.340.

[33] Z. Qin, G. Zuo, Y. Wang, H. Wu, G. Sun, and Y. Sun, "Electrohydraulic forming," in *High Voltage Strong Pulse Discharge its Application*, 1st ed. Beijing, China: Beijing Univ. Technology Press, 2000, pp. 61–74.

[34] Y. Wang, "Theoretical and experimental study of the underwater plasma acoustic source," Ph.D. dissertation, School Electron. Sci. Technol., Nat. Univ. Defense Technol., Changsha, China, 2012.

[35] A. P. Smirnov, V. G. Zhekul, and S. G. Poklonov, "The influence of the hydrostatic pressure on the parameters of a pressure wave generated by an electric discharge in a fluid," *Surf. Eng. Appl. Electrochemistry*, vol. 50, no. 3, pp. 233–237, May 2014, doi: 10.3103/S1068375514030077.

[36] Q.-X. Lin, L. Zhu, Z. He, X.-Y. Xu, J.-X. Liu, and J.-S. Chang, "The research on pulsed arc electrohydraulic discharge with discharge electrode and its application to removal of bacteria," *IEEE Trans. Plasma Sci.*, vol. 43, no. 4, pp. 1029–1039, Apr. 2015, doi: 10.1109/TPS.2015.2402164.

[37] G. Touya, T. Reess, L. Pécastaing, A. Gibert, and P. Domens, "Development of subsonic electrical discharges in water and measurements of the associated pressure waves," *J. Phys. D, Appl. Phys.*, vol. 39, no. 24, pp. 5236–5244, Dec. 2006, doi: 10.1088/0022-3727/39/24/021.

BIN LI received the B.E. degree from Henan Polytechnic University, in 2010, and the M.Sc. degree from the Southwest University of Science and Technology, in 2013. He is currently pursuing the Ph.D. degree with the Anhui University of Science and Technology. His research interests include safety science, coal mine safety, and the application of high-voltage electricity in mine disaster prevention and control.

SHENG XUE received the B.E. degree from the China University of Mining and Technology, in 1984, and the Ph.D. degree from the University of New South Wales Sydney (UNSW Sydney), in 1991. He is currently a Professor with the Anhui University of Science and Technology. He has published more than 140 research articles. His research interests include prevention and control of dynamic hazards in coal mining.

LIANG YUAN received the B.E. degree from the Huainan Institute of Mining (now Anhui University of Science and Technology), in 1982.

He is currently an Academician of the Chinese Academy of Engineering and a Professor and a Ph.D. Supervisor with the Anhui University of Science and Technology. His research interests include safe, intelligent and precision mining of coal, prevention and control of dynamic hazards and dust in coal mining, and occupational safety and health. He is also the President of the Anhui University of Science and Technology, and concurrently the Dean of the Anhui Research Institute of China Engineering Technology Development Strategy and the Vice Chairman of the Public Safety Science and Technology Society. He has presided over a number of scientific research projects at national, provincial and ministerial levels and enterprises. The research achievements have won six second prizes of National Science and Technology Progress Award, one Chinese Patent Gold Award, and nine provincial and ministerial levels science and technology progress special prize and first prize; and 72 national invention patents have been authorized, eight academic monographs have been published, and more than 100 academic articles have been published. It has won the "Outstanding Contribution Award" of the World Mining Congress, the Major Scientific and Technological Achievement Award of Anhui Province, the national outstanding scientific and technological workers, the young and middle-aged experts with outstanding contributions, and the national top-notch talents in coal system, and enjoys the special allowance of the State Council.

• • •